The effect of grain size on the sensitivity of nanocrystalline metal-oxide gas sensors

Cite as: Journal of Applied Physics **95**, 6374 (2004); https://doi.org/10.1063/1.1728314
Submitted: 26 January 2004 . Accepted: 09 March 2004 . Published Online: 25 May 2004

Avner Rothschild, and Yigal Komem

The effect of grain size on the sensitivity of nanocrystalline metal-oxide gas sensors

Avner Rothschild[a] and Yigal Komem
Faculty of Materials Engineering, Technion—Israel Institute of Technology, Haifa 32000, Israel

(Received 26 January 2004; accepted 9 March 2004)

The effect of grain size on the sensitivity of chemoresistive nanocrystalline metal-oxide gas sensors was evaluated by calculating the effective carrier concentration as a function of the surface state density for a typical sensing material, SnO_2, with different grain sizes between 5 and 80 nm. This involved numerical computation of the charge balance equation (the electroneutrality condition) using approximated analytical solutions of Poisson's equation for small spherical crystallites. The calculations demonstrate a steep decrease in the carrier concentration when the surface state density reaches a critical value that corresponds to a condition of fully depleted grains, namely, when nearly all the electrons are trapped at the surface. Assuming that the variations in the surface state density are induced by surface interactions with ambient gas molecules, these calculations enable us to simulate the response curves of nanocrystalline gas sensors. The simulations show that the conductivity increases linearly with decreasing trapped charge densities, and that the sensitivity to the gas-induced variations in the trapped charge density is proportional to $1/D$, where D is the average grain size. © *2004 American Institute of Physics.* [DOI: 10.1063/1.1728314]

I. INTRODUCTION

Semiconducting metal oxides such as SnO_2, TiO_2, and ZnO are used for gas sensing applications due to the sensitivity of their electrical conductivity to the ambient gas composition, which arises from charge transfer interactions with reactive gases such as O_2, NO_x, CO, hydrocarbons and volatile organic compounds.[1] The sensitivity to gases depends on the microstructure of the sensing material, especially on the porosity and grain size.[2,3] Xu *et al.*[4] reported that the gas sensitivity of sintered SnO_2 elements with ultrafine particles in the range of 4–27 nm increased steeply when the average crystallite size D was below about 10 nm, as shown in Fig. 1. One can see that when $D>20$ nm the sensor's response signal R_a/R_g (where R_a is the resistance measured in clean air and R_g is the resistance measured in air mixed with the test gas) is nearly independent of the grain size, but below about 20 nm it increases with decreasing grain size, where below about 10 nm this increase is remarkable. These results had a substantial impact on the design of metal-oxide gas sensors, leading to the development of various methods to produce sensors with a stable nanoporous microstructure.[5–7] However, the gas sensing mechanism of nanocrystalline metal oxides is unclear and the effect of grain size on the gas sensitivity in the limit of nanosized grains requires further clarification.[4]

To explain the effect of grain size on the sensitivity of metal-oxide gas sensors, Xu *et al.*[4] proposed a semiquantitative model which is depicted schematically in Fig. 2. According to their model the sensor consists of partially sintered crystallites that are connected to their neighbors by necks. Those interconnected grains form larger aggregates that are connected to their neighbors by grain boundaries (GB). Three different cases can be distinguished according to the relationship between the grain size D and the width of the depletion layer L that is produced around the surface of the crystallites due to chemisorbed adions (mostly oxygen adions, $O^-_{(ad)}$).[4] For large grains, i.e., when $D \gg 2L$, most of the volume of the crystallites is unaffected by the surface interactions with the gas phase, as depicted in Fig. 2(a). In this case the predominant effect of the ambient gas atmosphere on the sensor's conductivity is introduced via the GB barriers for intercrystallite charge transport from one grain (agglomerate) to another. The electrical conductivity σ depends exponentially on the barrier height $q|V_B|$: $\sigma \propto \exp(-q|V_B|/kT)$, where q is the elementary electron charge, V_B is the GB potential, k is Boltzmann's constant, and T is the temperature.[8] According to the depletion approximation $q|V_B| \propto (N_t^-)^2$, where N_t^- is the trapped charge density at the surface of the crystallites. N_t^- can be modified by charge transfer interactions with reactive gases such as O_2, NO_x, and CO,[9,10] and therefore the conductivity is sensitive to the ambient gas composition. Thus, for large grains ($D \gg 2L$) the gas sensing mechanism is controlled by the GB barriers. Furthermore, the GB barriers are independent of the grain size and therefore the sensitivity is independent of D.

As the grain size decreases the depletion region extends deeper into the grains and consequently the core region, which is relatively conductive with respect to the depletion region adjacent to the surface, becomes smaller. When D approaches but still larger than $2L$, i.e., when $D \geqslant 2L$, the depletion region that surrounds each neck forms a constricted conduction channel within each aggregate, as depicted in Fig. 2(b). Consequently, the conductivity depends

[a]Authorto whom correspondence should be addressed; Present address: Crystal Physics and Electroceramics Labarotary, Department of Materials Science & Engineering, MIT, Room No. 13-5126, Cambridge, MA 02139; electronic mail: avner@mit.edu

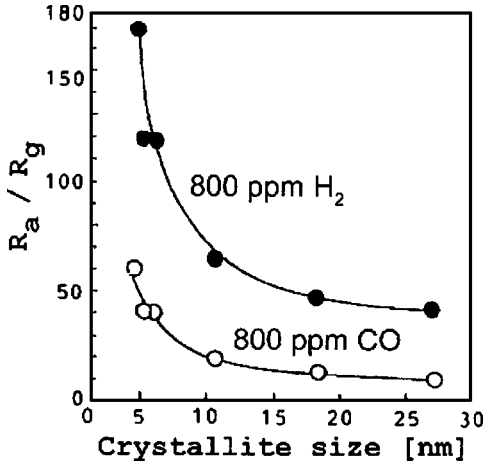

FIG. 1. The effect of crystallite size on the resistance of nanoporous SnO_2 elements upon exposure to 800 ppm of H_2 (●) or CO (○) in air at an operating temperature of 300 °C. Reprinted from Ref. 4 Copyright (1991), with permission from Elsevier.

not only on the GB barriers but also on the cross section area of those channels.[4] This area is proportional to $(X-L)^2$, where X is the neck diameter, which is proportional to the grain size D ($X \approx 0.8D$ according to Ref. 4). As a result, the conductivity is a function of the ratio X/L (or X/D). Since $L \propto N_t^-$ and N_t^- is modulated by the surface interactions with the gas phase, the effective cross section area of the current path though the grains is sensitive to the ambient gas composition. The current constriction effect adds up to the effect of the GB barriers, and therefore the gas sensitivity is enhanced with respect to the former case [$D \gg 2L$, cf. Fig. 2(a)]. Furthermore, the sensitivity to gases becomes grain size dependent and it increases when D decreases.[4]

When $D<2L$ the depletion region extends throughout the whole grain and the crystallites are almost fully depleted of mobile charge carriers, as shown in Fig. 2(c). As a result, the conductivity decreases steeply since the conduction channels between the grains are vanished. The energy bands are nearly flat throughout the whole structure of the interconnected grains,[11] and since there are no significant barriers for intercrystallite charge transport the conductivity is essentially controlled by the intracrystallite conductivity (grain controlled). It was found empirically that the highest gas sensitivity is obtained in this case, that is, when $D<2L$.[4] However, the gas sensing mechanism of such ultrafine particles is not clear, and the reason for the steep increase in the sensitivity with decreasing grain size even when D is already smaller than $2L$ needs further clarification.[4]

This paper presents a quantitative model that describes the effect of grain size on the sensitivity of metal-oxide gas sensors with nanosized grains in the limit of $D<2L$. The model is applied to nanocrystalline SnO_2 gas sensors by using simulations of the sensitivity as a function of the grain size, and the results are compared with experimental data given in the literature.[4]

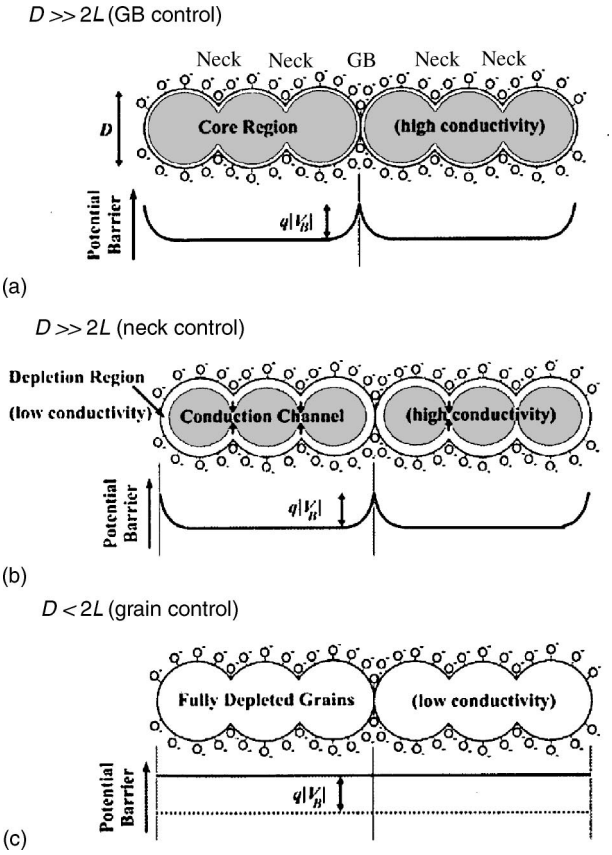

FIG. 2. Schematic model of the effect of the crystallite size on the sensitivity of metal-oxide gas sensors: (a) $D \gg 2L$ (GB control); (b) $D \geqslant 2L$ (neck control); (c) $D<2L$ (grain control).

II. MODEL

Similar to other chemical sensors, the sensing mechanism of metal-oxide gas sensors involves two functions: the *receptor function* that recognizes the target analyte by some sort of chemical interaction, and the *transducer function* that transforms the chemical signal into an electrical signal such as a change in the sensor's conductivity.[12] In the case of metal-oxide gas sensors the receptor function is provided by charge transfer interactions between the sensor and ambient gas molecules. These interactions largely involve chemisorption of oxygen adions, $1/2O_{2(g)} + e_{cb}^- \rightleftharpoons O_{(ad)}^-$ (where e_{cb}^- designates a conduction band electron), and removal of (some of) these adions by interactions with reducing gases such as CO, H_2, and hydrocarbons, e.g., $CO_{(g)} + O_{(ad)}^- \rightarrow CO_{2(g)} + e_{cb}^-$.[1,6,9] Normally the trapped charge density at the surface of the sensor largely depends on the density of chemisorbed oxygen adions, $N_t^- \approx [O_{(ad)}^-]$ (where the square brackets designate density per unit surface area), and therefore it is sensitive to the ambient gas composition due to interactions with gas molecules.

The dependence of the trapped charge density on the ambient gas composition is essentially described by the sensor's receptor function $\hat{f}_R: N_t^- = \hat{f}_R(p_{O_2}, p_{CO}, p_{H_2}, \ldots, T)$, where p_{O_2}, p_{CO}, and p_{H_2} are the partial pressures of the corresponding gases. The gas-induced variations in the trapped charge density are transformed into changes in the electrical conductivity by the sensor's transducer function, producing the sensor's output response signal. Thus, the transducer function $\hat{f}_T$ describes essentially the dependence

of the electrical conductivity on the trapped charge density, $\sigma=\hat{f}_T(N_t^-)$. Eventually, the overall response function of the sensor can be described as a superposition of the sensor's transducer and receptor functions, $\sigma=\hat{f}_T\otimes\hat{f}_R=f(N_t^-(p_{O_2}, p_{CO}, p_{H_2},\ldots,T))$. The relationship between N_t^- and the ambient gas composition, or in other words the sensor's receptor function, has already been described elsewhere (see Refs. 9 and 10). In this paper we focus on the transducer function of nanocrystalline metal-oxide gas sensors, aiming at describing the effect of grain size in the limit of nanosized grains where $D<2L$.

In order to study this effect we developed a computational method that enables us to calculate the conductivity as a function of the trapped charge density for nanosized grains. In this case where $D<2L$ the energy bands are nearly flat and there are no significant barriers for intercrystallite charge transport.[11] Thus, the conductivity is proportional to the effective carrier concentration n_{eff} in the crystallites,

$$\sigma\propto n_{\text{eff}}=\frac{1}{V}\int_V n(r)dV, \tag{1}$$

where V is the volume of the crystallite and $n(r)$ the local carrier concentration at a distance r from its center. $n(r)$ is a function of the electrostatic potential at point r,

$$n(r)=N_D\exp[-\phi(r)], \tag{2}$$

where N_D is the doping level and $\phi\equiv -q\varphi/kT$ is the reduced potential. φ is the electrostatic potential, which is negative ($\varphi<0$) for depletion layers. For simplicity we assume that the sensor can be treated approximately as a three-dimensional structure of interconnected spherical crystallites with radius R ($D=2R$ is the grain diameter, or in other words the grain size).

In order to calculate n_{eff} one should know the shape of the potential barrier $\phi(r)$ as a function of r. This can be derived by solving Poisson's equation and the charge neutrality condition. Poisson's equation in spherical coordinates is written as

$$\frac{1}{r^2}\frac{\partial}{\partial r}\left(r^2\frac{\partial\phi}{\partial r}\right)=\frac{1}{L_D^2}\{1-\exp[-\phi(r)]\}, \tag{3}$$

where $L_D=(\varepsilon kT/q^2N_D)^{1/2}$ is the Debye length and ε the dielectric constant. Due to their spherical symmetry the electric field must vanish at the center of the crystallites, therefore the first boundary condition is $\partial\phi/\partial r=0$ at $r=0$. The second boundary condition can be set as $\phi=\phi_0$ at $r=0$, where ϕ_0 is obtained by solving the electroneutrality condition as described below.

Analytical solutions of Eq. (3) can be obtained for two limiting cases: for weak potential ($\phi\ll 1$) and for strong potential ($\phi\gg 1$). Under weak potential conditions $(1-e^{-\phi})\approx\phi$ and the solution is

$$\phi(r)=\phi_0\frac{\sinh(r/L_D)}{(r/L_D)}, \tag{4}$$

while under strong potential conditions $(1-e^{-\phi})\approx 1$ and the solution is

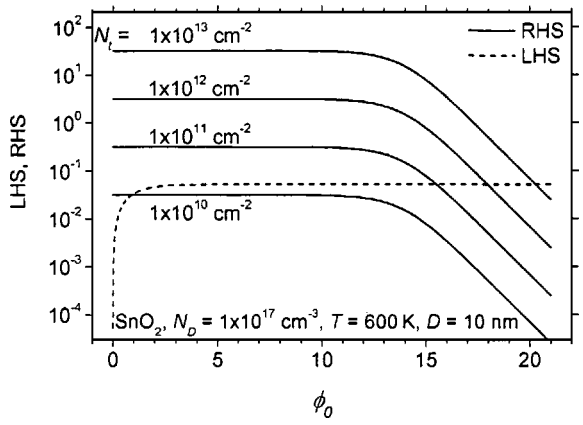

FIG. 3. Graphical solution of the charge balance equation [Eq. (6)]. The left-hand side (LHS) and right-hand side (RHS) of Eq. (6) are plotted as a function of ϕ_0 and the solution is given by the intersection of these curves.

$$\phi(r)=\phi_0+\frac{1}{6}\left(\frac{r}{L_D}\right)^2. \tag{5}$$

In order to calculate the potential ϕ_0 at the center of the crystallites one should solve the charge balance equation

$$\int_V[N_D-n(r)]dV=4\pi R^2N_t^-, \tag{6}$$

where N_t^- is the density of occupied surface states (filled traps). Equation (6) describes the electroneutrality condition, which requires that the number of electrons withdrawn from the crystallite is equal to the number of electrons trapped on its surface.

The trapped charge density N_t^- depends on the density of both occupied and unoccupied states (N_t), and on the energy level of these states (E_t) with respect to the Fermi energy E_F at the surface,

$$N_t^-=\frac{N_t}{1+2\exp[(E_t-E_F)/kT]_{r=R}}. \tag{7}$$

It is worth noting that $(E_t-E_F)_{r=R}=(E_t-E_F)_{\phi=0}+kT\phi_s$, where $\phi_s\equiv\phi(r=R)$ is the surface potential. Therefore, N_t^- depends on ϕ_0 via Eq. (4) or (5). Thus, the left-hand side (LHS) and the right-hand side (RHS) of Eq. (6) are both functions of ϕ_0, which can be determined univocally by solving Eq. (6) numerically.

A graphical solution is demonstrated in Fig. 3, where the pertinent solution is obtained from the intersection of the curves describing the LHS and RHS of Eq. (6) as a function of ϕ_0. After obtaining the solution ϕ_0 the shape of the potential barrier $\phi(r)$ is readily obtained by substituting ϕ_0 into Eq. (4) or (5), depending on whether $\phi_0<1$ or $\phi_0>1$, respectively. Subsequently, the effective carrier concentration n_{eff} can be calculated numerically using Eq. (1). In order to study the effect of the ambient gas composition on the electrical conductivity these calculations can be carried out as a function of the surface state density N_t, which is largely controlled by surface interactions between the sensor and ambient gas molecules.

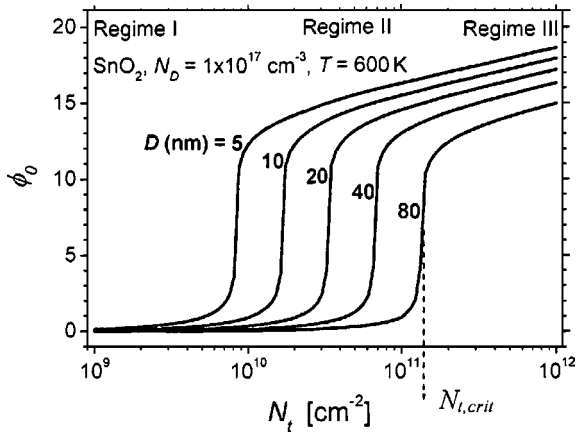

FIG. 4. The potential ϕ_0 as a function of the surface state density for SnO_2 with different grain sizes as indicated in the figure.

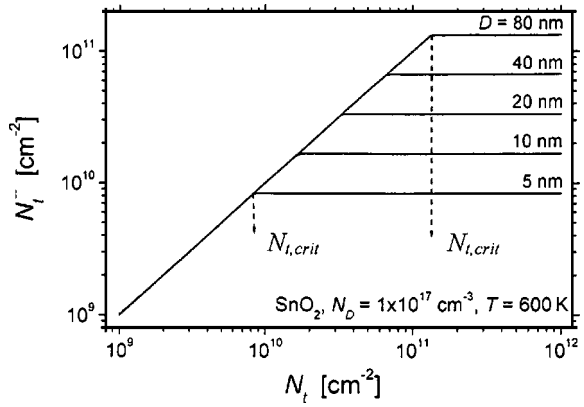

FIG. 6. The trapped charge density (occupied states) as a function of the surface state density (occupied and unoccupied states) for SnO_2 with different grain sizes as indicated in the figure.

III. NUMERICAL SIMULATIONS

To examine the effect of grain size on the sensitivity of nanocrystalline metal-oxide gas sensors we calculated the effective carrier concentration n_{eff} as a function of the surface state density N_t for nanosized SnO_2 crystallites with different grain size between 5 and 80 nm. The calculations were carried out using the computational method that was described in the preceding section. The physical parameters that were used represent typical values for SnO_2 gas sensors: $T=600$ K, $N_D=1\times10^{17}$ cm^{-3}, $\varepsilon=1\times10^{-12}$ F/cm, and $(E_C-E_t)_{\phi=0}=1$ eV (where E_C is the conduction band edge).[13–15] The corresponding Debye length L_D is 18.5 nm. The energy level of the trapping states corresponds to oxygen chemisorbates on SnO_2.[15] It is worth noting that different gas species might have different electron affinities and therefore the corresponding energy level could vary from one gas to another.

Figures 4 and 5 depict the results of the calculations of the potential ϕ_0 and the effective carrier concentration n_{eff} as a function of the surface state density N_t, respectively. Three characteristic regimes can be observed in both figures, and the transition from one regime to another depends on the grain size. At low surface state densities (regime I) ϕ_0 increases and n_{eff} decreases rather moderately with increasing N_t. But when N_t reaches a critical value $N_{t,crit}$ a sharp increase in ϕ_0 takes place while the carrier concentration n_{eff} decreases by several orders of magnitude (regime II). At high surface state densities ($N_t>N_{t,crit}$), ϕ_0 increases and n_{eff} decreases rather moderately with increasing N_t (regime III). A very interesting result that emerged from these calculations regards the effect of grain size. Both Figs. 4 and 5 show that with increasing grain size the transition from regime I to regime II shifts to higher surface state densities. In other words, the larger is the grain size the higher is $N_{t,crit}$.

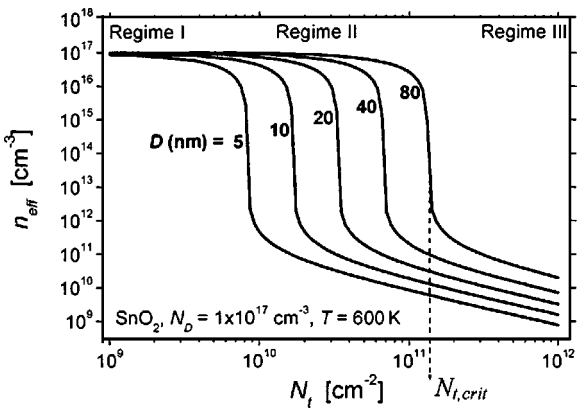

FIG. 5. The effective carrier concentration as a function of the surface state density for SnO_2 with different grain sizes as indicated in the figure.

The significance of $N_{t,crit}$ is highlighted in Fig. 6, which gives plots of the trapped charge density N_t^- (occupied surface states) as a function of the surface state density N_t (both occupied and unoccupied states). One can see that when $N_t<N_{t,crit}$ nearly all states are occupied and $N_t^-\approx N_t$. This is because at low surface state densities the surface potential ϕ_s is small (see Fig. 4), and since the states lay deep ($\sim$1 eV) below the Fermi energy their occupation probability is close to unity. But when the critical point is reached ($N_t=N_{t,crit}$) the surface potential increases significantly (Fig. 4) and consequently E_t shifts upwards and almost levels with E_F. In other words, the Fermi energy is pinned at E_t. As a result, the occupation probability decreases and the trapped charge density saturates and practically does not change at higher surface densities. The simulations indicate that the saturation occurs when $N_t=N_{t,crit}=DN_D/6$ and $N_t^-\approx DN_D/6$. Given the fact that $D/6$ is the volume to surface ratio for spherical crystallites with grain size D, it is concluded that the saturation occurs when nearly all electrons are trapped at the surface.

It should be noted though that N_t^- still slightly increases with N_t even beyond the critical point ($N_t>N_{t,crit}$), but these very small changes cannot be resolved in Fig. 6. However, they still lead to observable changes in the effective carrier concentration, as shown in Fig. 5 (regime III). This is because the effect of the variations in the trapped charge density on the carrier concentration is multiplied by the surface to volume ratio, $6/D$, which is a very high factor in nanocrystalline materials.

IV. DISCUSSION

The numerical simulations depicted in the preceding section (cf. Figs. 4–6) show that in nanocrystalline metal-oxide gas sensors the grain size has a crucial effect on the effective carrier concentration and consequently on the electrical conductivity. Further discussion of the effect of grain size on the sensitivity to gases requires clear definitions of the main sensor characteristics: the *output response signal* $\Re$ and the *sensitivity S*. The output response signal, $\Re=\sigma/\sigma_0$, is the ratio of the conductivity measured during exposure to the test gas (σ) and the conductivity measured under the baseline conditions (σ_0), which normally means in clean air at atmospheric pressure. A plot of the response signal as a function of the gas composition (or in other words the concentration C of the test gas) is the sensor's response curve, and the sensitivity is defined as the slope of this curve, $S=\partial\Re/\partial C$.[16]

In metal-oxide gas sensors the variations in the ambient gas composition modify the trapped charge density N_t^-.[10] As mentioned above, this is largely due to interactions between the analyte gas molecules and preadsorbed oxygen adions ($O_{(ad)}^-$). For instance, CO molecules interact with preadsorbed oxygen adions and oxidize to CO_2 molecules, $CO_{(g)}+O_{(ad)}^-\rightarrow CO_{2(g)}+e_{cb}^-$.[17] As a result, the chemisorption-induced trapped charge density decreases, and electrons that were trapped in oxygen adions are liberated and return as free electrons (e_{cb}^-) to the conduction band. Thus, N_t^- depends on the gas concentration C.

The relationship between N_t^- and C was described elsewhere (see Refs. 9 and 10). It relates to the receptor function of the sensor, whereas in the present work we are mostly interested in the transducer function. In order to distinguish between the two functions we define the *normalized sensitivity* $\hat{S}=-\partial(\sigma/\sigma_0)/\partial(N_t^-/N_{t,0}^-)$, where $N_{t,0}^-$ is the trapped charge density in clean air, that is, under the baseline conditions. Namely, σ and N_t^- are the conductivity and trapped charge density during exposure to the test gas, respectively, whereas σ_0 and $N_{t,0}^-$ are the corresponding values under the baseline conditions. The minus sign is due to the fact that N_t^- decreases when C increases. The advantage of this approach, which was originally proposed by Vlachos and Papadopoulos,[18] is that it circumvents the need to know the exact relationship between N_t^- and C, which may vary from one gas to another. Thus, it enables us to deal exclusively with the transducer function of the sensor without being concerned about the specific details of the chemical reactions that control its receptor function. The underlying assumption is that an isothermal change in the gas concentration always leads to the same modification in the normalized trapped charge density (for a given semiconductor/gas system).

Using the data from the simulations in the preceding section, Fig. 7 describes the respective normalized response curve, wherein $\Re=\sigma/\sigma_0=n_{\text{eff}}/n_{\text{eff},0}$ is plotted as a function of the normalized trapped charge density $N_t^-/N_{t,0}^-$. $n_{\text{eff},0}$, and $N_{t,0}^-$ are the corresponding values when $N_t=10^{12}\ \text{cm}^{-2}$, which is approximately the chemisorption-induced surface state density in atmospheric air.[10] One can see that the response signal increases linearly with decreasing values of the normalized trapped charge density, and it follows a linear relationship of the form $y=\hat{S}(1-x)+1$, where $y\equiv n_{\text{eff}}/n_{\text{eff},0}$ is the normalized response and $x\equiv N_t^-/N_{t,0}^-$ the normalized trapped charge density. The slope $\hat{S}$, i.e., the normalized sensitivity, increases when the grain size decreases, as shown in the inserted table in Fig. 7. Specifically, $\hat{S}$ was found to be proportional to $1/D$, as depicted in Fig. 8. This is the most important conclusion derived from our simulations. In order to verify it we reevaluated the experimental results reported by Xu *et al.*[4] (cf. Fig. 1) to check whether they follow this relationship. Indeed, Fig. 9 confirms that the measured response $\Re=R_a/R_g(=\sigma_g/\sigma_a)$, upon exposure to 800 ppm of H_2 (●) or CO (○) behaves as a linear function of $1/D$, in accord with our simulations. This important result suggests that the sensitivity is proportional to the surface to volume ratio, i.e., to $6/D$ in the case of spherical crystallites.

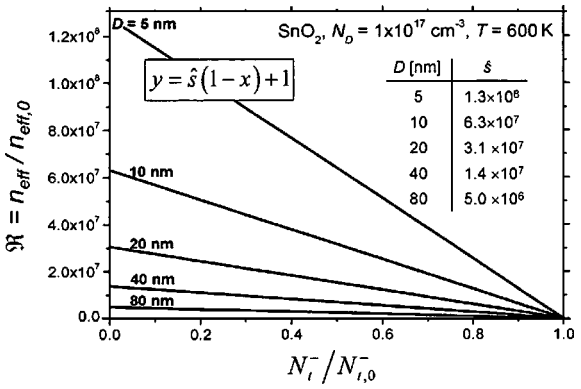

FIG. 7. The normalized response curves calculated for SnO_2 with different grain sizes as obtained from the simulations presented in Figs. 5 and 6.

According to Fig. 7 the response signal $\Re=n_{\text{eff}}/n_{\text{eff},0}$ can be as high as $\sim 10^7$ when the normalized trapped charge is reduced significantly (by 10–20%). In reality, however, the response signal of nanocrystalline SnO_2 gas sensors is typically of the order of 10^1-10^2, and it seldom reaches the 10^3-10^4 range.[19,20] The apparent discrepancy between our simulations and the empirical results can be attributed to the fact that in reality the gas-induced variations in the trapped charge density are very small, probably of the order of about

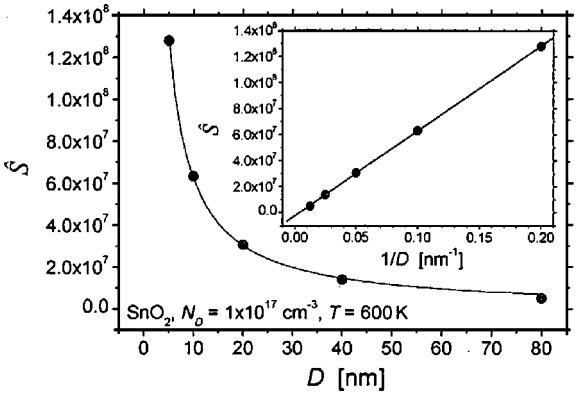

FIG. 8. The normalized sensitivity, $\hat{S}=-\partial(n_{\text{eff}}/n_{\text{eff},0})/\partial(N_t^-/N_{t,0}^-)$, as a function of the grain size D as obtained from Fig. 7. The inset shows $\hat{S}$ as a function of $1/D$.

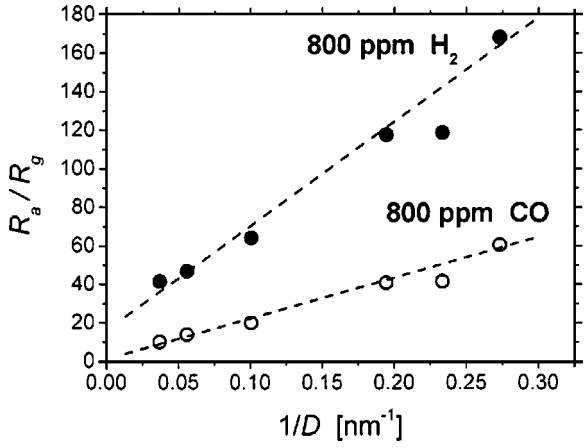

FIG. 9. The response of nanoporous SnO_2 elements to 800 ppm of H_2 (●) or CO (○) in air at an operating temperature of 300 °C as a function of $1/D$. The experimental data are taken from Ref. 4 (see also Fig. 1).

1–10 ppm. This is because the variations in the ambient gas composition are also very small. Under typical conditions the gas sensor is exposed to gas concentrations of the order of 1–10 ppm in otherwise clean air at atmospheric pressure. Therefore, it is reasonable to expect that the gas-induced variations in the trapped charge density should have about the same magnitude as the variations in the ambient gas composition. Taking this into account our simulations yield much more reasonable values. For instance, Fig. 10 shows the calculated response as a function of the grain size when the variation in the trapped charge density is 1 ppm, i.e., when $N_t^-/N_{t,0}^- = 1 - 10^{-6} = 99.9999\%$. The corresponding response signal $\Re = n_{\mathrm{eff}}/n_{\mathrm{eff},0}$ is equal to 129 for the smallest crystallites ($D = 5$ nm) and it drops to lower values for larger crystallites. These values are in line with the typical response signals of nanocrystalline SnO_2 gas sensors.[4,19,20]

V. SUMMARY AND CONCLUSIONS

A quantitative model of the transducer function of nanocrystalline metal-oxide gas sensors was described. The model includes a method for calculating the effective carrier concentration in nanosized crystallites under conditions where the entire volume of the crystallite is depleted of mobile carriers due to electron trapping at surface states. This enables us to calculate the effect of the gas-induced variations in the surface state density on the electrical conductivity of nanosized crystallites with different grain sizes. Consequently, one can evaluate the effect of grain size on the sensitivity of nanocrystalline metal-oxide gas sensors, as was demonstrated in this work.

Using this method, the effective carrier concentration of nanosized SnO_2 crystallites was calculated as a function of the surface state density for different grain sizes between 5 and 80 nm. The simulations demonstrate a steep decrease in the carrier concentration when the surface state density reaches a critical value that corresponds to a condition of fully depleted grains, that is, when nearly all the electrons are trapped at the surface of the crystallites. This critical value was found to be proportional to the grain size D.

Assuming that the variations in the surface state density are induced by chemisorption and surface interactions with ambient gas molecules, the simulations enable us to evaluate the normalized response curves of SnO_2 gas sensors with similar properties (grain size, doping level, temperature, etc.). They show that in nanosized crystallites even very small variations (~1 ppm) in the trapped charge density lead to significant changes in the effective carrier concentration and the electrical conductivity. This implies that in nanocrystalline gas sensors the gas-induced variations in the trapped charge density are greatly amplified by the sensor's transducer function. Furthermore, it was found that the sensitivity is proportional to $1/D$, and it was shown that the experimental data for nanosized SnO_2 gas sensors follow a similar relationship. This suggests that the amplification power of the sensor's transducer function, which transforms the interactions between the sensor and the gas phase into an electrical signal (i.e., a conductivity change), is proportional to the surface to volume ratio of the sensor material. This result has important implications on the design of metal-oxide gas sensors for optimizing their gas sensitivity.

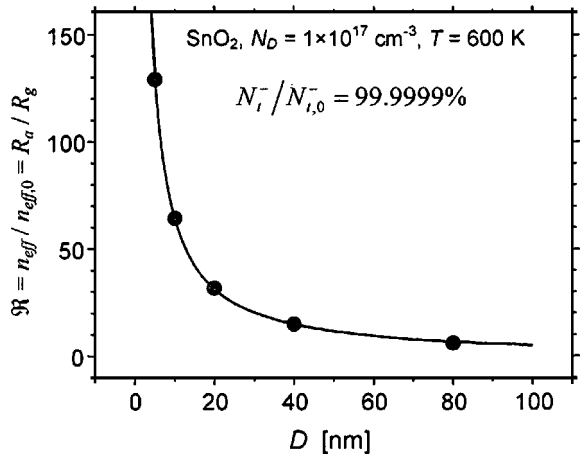

FIG. 10. The calculated response signal $\Re = n_{\mathrm{eff}}/n_{\mathrm{eff},0}$ as a function of the grain size D for a small variation in the trapped charge density ($N_t^-/N_{t,0}^- = 1 - 10^{-6} = 99.9999\%$). Based on results from Fig. 7.

ACKNOWLEDGMENTS

A.R. would like to thank the Israeli Ministry of Science for the Eshkol fellowship and the Israeli Council for Higher Education for the VATAT fellowship. Y.K. would like to thank the Fund for the Promotion of Research at the Technion for partial support.

[1] M. J. Madou and S. Y. Morison, *Chemical Sensing with Solid State Devices* (Academic Press, San Diego, 1989).
[2] H. Ogawa, A. Abe, M. Nishikawa, and S. Hayakawa, J. Electrochem. Soc. **128**, 2020 (1981).
[3] H. Ogawa, M. Nishikawa, and A. Abe, J. Appl. Phys. **53**, 4448 (1982).
[4] C. Xu, J. Tamaki, N. Miura, and N. Yamazoe, J. Electrochem. Soc. Jpn. **58**, 1143 (1990); Sens. Actuators B **3**, 147 (1991).
[5] G. Sberveglieri, Sens. Actuators B **6**, 239 (1992).
[6] N. Barsan, M. Schweizer-Berberich, and W. Göpel, Fresenius' J. Anal. Chem. **365**, 287 (1999).
[7] M. K. Kennedy, F. E. Kruis, H. Fissan, B. R. Mehta, S. Stappert, and G. Dumpich, J. Appl. Phys. **93**, 551 (2003).
[8] G. Martinelli and M. C. Carotta, Sens. Actuators B **23**, 157 (1995).

[9] N. Barsan and U. Weimar, J. Electroceramics **7**, 143 (2001).
[10] A. Rothschild, Y. Komem, and N. Ashkenasy, J. Appl. Phys. **92**, 7090 (2002); A. Rothschild and Y. Komem, Sens. Actuators B **93**, 362 (2003).
[11] J. W. Orton and M. J. Powell, Rep. Prog. Phys. **43**, 1263 (1980).
[12] N. Yamazoe, Sens. Actuators **5**, 7 (1991).
[13] S. R. Morrison, Sens. Actuators B **2**, 329 (1982).
[14] Z. M. Jarzebski and J. P. Marton, J. Electrochem. Soc. **123**, 333C (1976).
[15] V. Lantto and P. R. Romppainen, Surf. Sci. **192**, 243 (1987).
[16] A. D'Amico and C. Di Natale, IEEE Sensors J. **1**, 183 (2001).
[17] H. Windischmann and P. Mark, J. Electrochem. Soc. **126**, 627 (1979).
[18] D. S. Vlachos, C. A. Papadopoulos, and N. J. Avaritsiotis, J. Appl. Phys. **80**, 6050 (1996).
[19] Y. Shimizu and M. Egashira, MRS Bull. **24**, 18 (1999).
[20] S. Seal and S. Shukla, JOM **54**, 35 (2002).